(2)

TECHNICAL REPORT BRL-TR-3352

BRL

TRIPLE QUADRUPOLE MASS SPECTROMETRY DIAGNOSTICS OF PROPELLANT-LIKE FLAMES

STEPHEN L. HOWARD
JOYCE E. NEWBERRY
ROSARIO C. SAUSA
ANDRZEJ W. MIZIOLEK

JUNE 1992

U.S. ARMY LABORATORY COMMAND

BALLISTIC RESEARCH LABORATORY
ABERDEEN PROVING GROUND, MARYLAND

NOTICES

Destroy this report when it is no longer needed. DO NOT return it to the originator.

Additional copies of this report may be obtained from the National Technical Information Service, U.S. Department of Commerce, 5285 Port Royal Road, Springfield, VA 22161.

The findings of this report are not to be construed as an official Department of the Army position, unless so designated by other authorized documents.

The use of trade names or manufacturers' names in this report does not constitute indorsement of any commercial product.

REPORT DOCUMENTATION PAGE

Form Approved
OMB No. 0704-0188

1. AGENCY USE ONLY *(Leave blank)*	2. REPORT DATE	3. REPORT TYPE AND DATES COVERED
	June 1992	Final, June 1991–October 1991

4. TITLE AND SUBTITLE

Triple Quadrupole Mass Spectrometry Diagnostics of Propellant-Like Flames

5. FUNDING NUMBERS

PR: 1L161102AH43

6. AUTHOR(S)

Stephen L. Howard, Joyce E. Newberry, Rosario C. Sausa, and
Andrzej W. Miziolek

7. PERFORMING ORGANIZATION NAME(S) AND ADDRESS(ES)

U.S. Army Ballistic Research Laboratory
ATTN: SLCBR-IB-P
Aberdeen Proving Ground, MD 21005-5066

8. PERFORMING ORGANIZATION REPORT NUMBER

9. SPONSORING/MONITORING AGENCY NAME(S) AND ADDRESS(ES)

U.S. Army Ballistic Research Laboratory
ATTN: SLCBR-DD-T
Aberdeen Proving Ground, MD 21005-5066

10. SPONSORING/MONITORING AGENCY REPORT NUMBER

BRL-TR-3352

11. SUPPLEMENTARY NOTES

12a. DISTRIBUTION/AVAILABILITY STATEMENT

Approved for public release; distribution is unlimited.

12b. DISTRIBUTION CODE

13. ABSTRACT *(Maximum 200 words)*

A new research apparatus for characterization of low-pressure premixed flames has been developed and was used to characterize the $C_2H_4/N_2O/Ar$ flame at 20 Torr. This instrument incorporates several diagnostic techniques in one apparatus so that individual techniques can be quantitatively compared and the usable detection range (both in terms of resolution and species detection) expanded. Results discussed in this report include mass analysis by triple quadrupole mass spectrometer and temperature measurement by thermocouple. Concentration profiles in the one-dimensional flame include CO, N_2, and C_2H_4 at nominal m/z = 28 as well as CO_2 and N_2O at m/z = 44.

14. SUBJECT TERMS

flames, mass spectrometry, collision-induced dissociation, mass spectrometers

15. NUMBER OF PAGES

39

16. PRICE CODE

17. SECURITY CLASSIFICATION OF REPORT	18. SECURITY CLASSIFICATION OF THIS PAGE	19. SECURITY CLASSIFICATION OF ABSTRACT	20. LIMITATION OF ABSTRACT
UNCLASSIFIED	UNCLASSIFIED	UNCLASSIFIED	UL

INTENTIONALLY LEFT BLANK.

TABLE OF CONTENTS

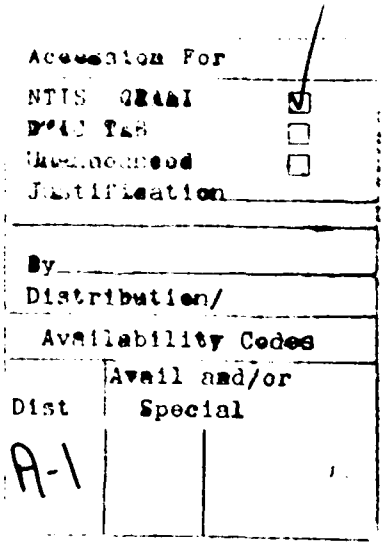

INTENTIONALLY LEFT BLANK.

LIST OF FIGURES

INTENTIONALLY LEFT BLANK.

ACKNOWLEDGEMENTS

This work was supported in part by the Office of Naval Research (ONR Contract No. 00001491MP24001) and by the BRL Combustion mission program. Support from the NRC/BRL Postdoctoral Research Program (SLH) is gratefully acknowledged.

INTENTIONALLY LEFT BLANK.

1. INTRODUCTION

Various laser spectroscopic techniques have been developed that work in the flame environment as diagnostics in determining the components and reaction mechanisms in propellant flames. Laser-induced fluorescence (LIF) and multiphoton techniques such as resonance-enhanced multiphoton ionization (REMPI) have yielded measurements with a good degree of selectivity and spatial resolution (Lucht et al. 1983, Alden et al. 1982, Goldsmith 1983). More intrusive techniques for gas sampling that use gas-liquid chromatography (GC) or mass spectrometry (MS) as detectors have also been used (Eltenton 1947, Serry and Zabielski 1989, Biordi et al. 1974, Greene and Pust 1958, Fristrom and Westenberg 1965, Banna 1979). As with the laser-based techniques, these techniques have advantages for some flame species and flame conditions and disadvantages for others. While study of ions produced in a flame is a long-investigated problem (Knewstubb and Sugden 1958) and mass spectrometry of flame neutrals had early beginnings (Eltenton 1947), the bulk of the subsequent research is more recent (Serry and Zabielski 1989, Biordi et al. 1974, Revet et al. 1978, Smith 1981, Smith and Chaudler 1986). As a result, the recent studies reflect the new technologies and methods that have been developed over the years that facilitate the identification and quantification of flame species.

Gas sampling by quartz microprobe (Greene and Pust 1958, Fristrom and Westenberg 1965, Banna 1979, Colket, III et al. 1982) has been shown to be adequate for stable species and therefore well-suited for GC studies. However, large residence times at significient pressures in the probe preclude this technique for reactive species. Most mass spectrometry studies of radical intermediates have been done by molecular-beam sampling techniques; indeed, the supersonic jet that forms the molecular beam is essential in preserving the

radicals until they can be ionized. Comparison of OH radical concentration profiles determined by optical methods with those determined by molecular-beam mass spectrometry (MB/MS) has shown that minor perturbations of the preheat zone occur but that flame front zone and post-flame regions are relatively undisturbed (Seery and Zabielski 1989, Revet et al. 1978, Howard et al. 1992a). In order to more fully characterize the possible operating range of each technique and to quantitatively compare results between techniques, a hybrid instrument for analysis of flames under the same operating conditions was developed. Previous work (Howard et al. 1992b) with $C_2H_4/O_2/Ar$ flames at 20 Torr with the present instrument showed that laser-based diagnostics for this simple flame were most appropriate for analysis close to the burner surface (0-2 mm), but that MB/MS possessed better qualities in the other regions of the flame. For example, molecular-beam mass spectrometry was able to investigate many more species concurrently (resulting in shorter scan times that permitted more scans to be performed) and also able to provide greater detail for some species higher in the reaction zone. Both methods appeared to be equivalent, for all cases where comparison could be made, in the burnt gas region far removed from the burner surface. It was concluded that in the current instrument, MB/MS, while not immune to quartz sampler perturbation, adequately describes nascent chemistry in the flame environment.

The current study ($C_2H_4/N_2O/Ar$), while relatively simple in terms of reactants and major products, includes unsaturated hydrocarbon oxidation and the more complex nitrogen flame chemistry present in many propellant (where oxides of nitrogen are primary oxidizers) and air-breathing flames. Inclusion of temperature measurements permits correlation with the concentration profiles in assisting to optimize thermal versus environmental concerns as well as to provide thermodynamic/kinetic data necessary for theoretical model evaluation.

2. EXPERIMENTAL

2.1 Sampling System.* All of the flames in this study were operated at 20.0 Torr absolute pressure. The instrument has been described earlier (Howard et al. 1992a) and only its salient components are mentioned here. The low-pressure burner chamber was a stainless steel cylinder with an inside nominal diameter of 25 cm and a height of 40 cm. Provision for temperature measurement by thermocouple [125-micron diameter platinum/platinum-10% rhodium wire coated with a noncatalytic beryllium/yttrium oxide mixture (Kent 1970)] was provided as shown in Figure 1.

The mass spectrometer consisted of an Extrel C50 TQMS inline triple quadrupole mass filter with a concentric-axis ionizer as shown schematically in Figure 1. Sampling of the flame gases occurred through a conical quartz skimmer with a 250-micron diameter orifice. The gases expanded supersonically into the first differential vacuum chamber with a measured average chamber pressure of 5×10^{-5} Torr. The expanding gases were then formed into a supersonic beam by collimation through a second skimmer (Beam Dynamics Model 2, orifice diameter 2 mm) and introduced into the ionization region of the first quadrupole (the first set of quadrupoles were used for mass analysis except where noted). This region was maintained at 1×10^{-6} Torr. The beam was then modulated at 200 Hz with a tuning fork chopper and ionized prior to entering the first quadrupole. The electron emission current was maintained at 0.10 ±0.01 mA and the nominal energy at 17.0 ±0.1 eV (0.5 eV FWHM) unless otherwise noted. The drawout voltage from the ionizer was set to between 0 and 1 Volt. These ionizing conditions optimized and stabilized the modulated beam. A beamstop was included to determine if the modulated beam was a molecular beam (modulation

* Useage of manufacturer name or model does not constitute endorsment of the product by the US Government or its affiliates.

would cease with beamstop activated) or an effusive beam (no change in modulation noted with beamstop activated). After traversing the quadrupoles the ion current was detected with a continuous-dynode electron multiplier. Amplified current from the detector then was processed with a Stanford Research System Model SR530 lock-in amplifier to discriminate signal from background gases and to signal average in order to increase sensitivity.

The flame was produced upon and supported by a 6-cm diameter flat burner (McKenna Products). Under proper gas flow conditions the flame was produced in a laminar flow field with the

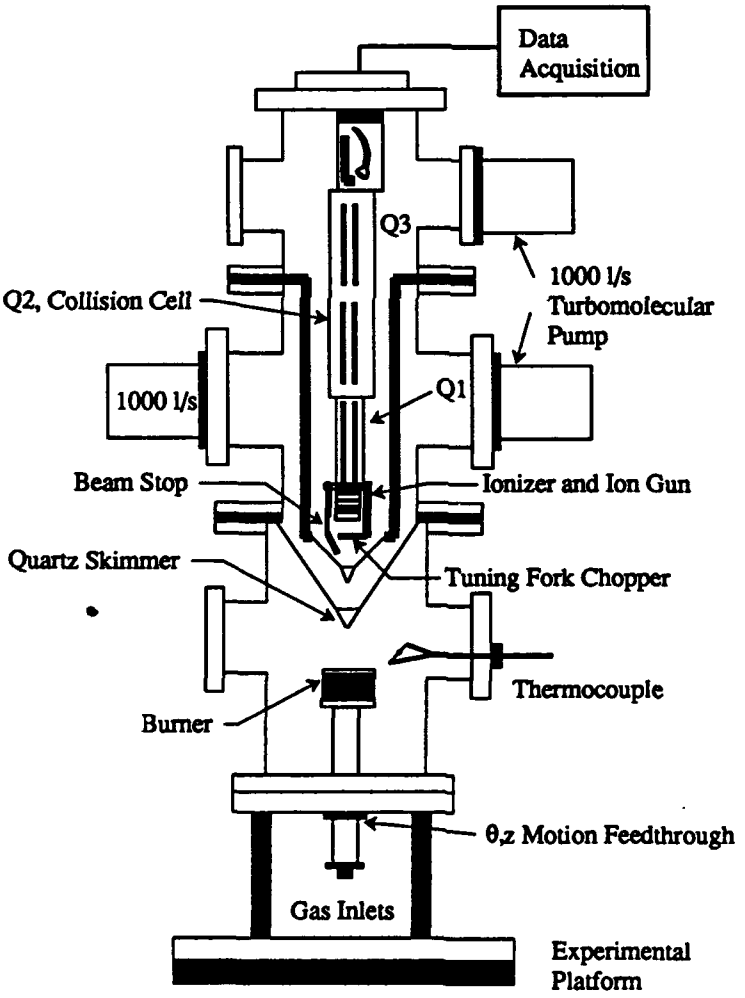

Figure 1. Schematic of Triple Quadrupole Mass Spectrometer and Molecular Beam System of the Experimental Apparatus.

flame front parallel to the burner surface and therefore one-dimensional with respect to the burner surface. Subsequently, the distance from the burner surface to a sampling point in the flame can be used as the reaction coordinate to describe the progress of reaction in terms of species concentration profiles as well as temperature profiles. In order to increase the spatial resolution the flame was operated at reduced pressure. Low-pressure (or subatmosphere) flames have shown that the reaction zones expand with minimal distortion as pressure is reduced (Gaydon and Wolfhard 1949, Salmon and Laurendeau 1987).

The reactant gases were of commercial high-purity grade and were metered by mass flow controllers (MKS Instruments, Inc) and premixed in the burner prior to passing through the flat 6-cm diameter sintered stainless steel plug in the center of the burner surface. Gas flows of C_2H_4, N_2O and Ar of 0.53, 3.2, and 1.0 liter (STP)/min, respectively, were used which resulted in linear flow rates on the order of 110 cm/sec with a Reynolds number on the order of 150 indicating operation well within the laminar regime. These flow rates corresponded to a stoichiometric, $\Phi = 1.0$ (Φ defined as the ratio of initial moles of fuel to oxidizer divided by the ratio of the respective stoichiometric coefficients), flame. The sintered stainless steel frit was water cooled to maintain a constant temperature as measured by imbedded Alumel-Chromel thermocouples. This central frit was encircled by another sintered metal frit through which argon was flowed, thus forming a protective shroud that minimized mixing of any recirculating burnt gases in the low-pressure chamber. The burner was mounted normal to the center of the burner chamber on a high-vacuum feedthrough flange that was coupled to a θz-translation stage. This stage allowed independent horizontal scanning (precision in θ of less than one degree) of the burner and vertical motion (precision on the order of 50 micron) allowed the diagnostics to remain stationary while "scanning" the flame (scanning the distance between the diagnostics and the burner surface).

2.2 Calibration Procedure. Several problems exist with using a moderately low resolution mass spectrometer with electron-impact ionization as the detector of flame species. For example, the ionization technique is not "soft" (i. e., fragmentation patterns occur for virtually every polyatomic species) and final ion currents depend heavily on ionization potentials and cross sections. For stable species this problem was addressed by preparing calibration gas mixtures that were introduced into the burner chamber at flame conditions. The nominal ionization energy of the electron beam during calibration was maintained at 17.0 eV (this value was chosen since it is below the ionization energy at which OH is produced from H_2O, yet above that required to ionize Ar). At this energy fragmentation of the primary ion beam was small.

All of the calibration mixtures contained argon (used in all the flames to dilute the flame and to increase spatial resolution). Since it is not produced or consumed in the flame and its ionization cross section is little affected at flame temperatures, it was considered as an ideal internal standard. As the observed mass spectrum signal can be described as:

$$I_i = S_i X_i \qquad (1)$$

where I_i is the observed ion current, S_i is a sensitivity factor (with appropriate units) containing instrument and ionization dependent information and X_i the mole fraction, partial pressure or other relevant concentration unit for the i-th component, the ratio of S_i to the sensitivity factor of an internal standard (such as argon),

$$K_i = S_i/S_{Ar} , \qquad (2)$$

may be used in the following manner to quantify the amount of the i-th component present:

$$X_i = X_{Ar}\left(\frac{I_i}{I_{Ar}}\right)\frac{1}{K_i} \quad . \qquad (3)$$

The validity of Equations 2 and 3 was verified in the flame by first measuring S_{He}/S_{Ar} at ambient temperature and 20 Torr pressure with a known mixture of helium and argon. This ratio was then measured under flame conditions by introducing a known concentration of He in the argon flow. Measurements were taken at various points from the burner surface through the flame front and into the burnt gas region. The assumption of one-dimensionality was also tested by horizontally scanning across the flame at each point. The radially measured ratios were the same within experimental error in all cases thereby verifying the the above assumptions.

Another problem arose with use of only moderate mass resolution. Several molecules may exhibit the same nominal mass-to-charge-ratio. CO_2 and N_2O were a case in point. Differentiation of such species pairs was possible with the triple quadrupole mass spectrometer through the use of collision-induced dissociation (CID) of the ions in the primary ion beam to produce fragmentation patterns unique to each molecule studied. The first quadrupole selected ions of interest in the ionized beam. These ions then passed through the rf-only quadrupole where collision with argon maintained at a pressure near 10^{-3} Torr occurred. Upon collision the selected ions fragmented and the daughter fragments were analyzed in the third quadrupole. Calibration gas mixtures of each gas with argon and also with each species possible at a given m/z of interest were prepared and the fragmentation patterns and branching ratios obtained.

Such calibration procedures were performed only for stable gases. Radicals and reactive intermediates require other techniques (where possible) for quantification. Therefore only relative profiles were obtained in this study for these species. However, at a

particular m/z value when more than one species was possible, CID was used to determine the respective contributions.

3. RESULTS AND DISCUSSION

3.1 The $C_2H_4/N_2O/Ar$ Flame. In this report we show temperature (Figure 2) and mass spectrometric measurements of many of the reactive and stable flame species in a stoichiometric,

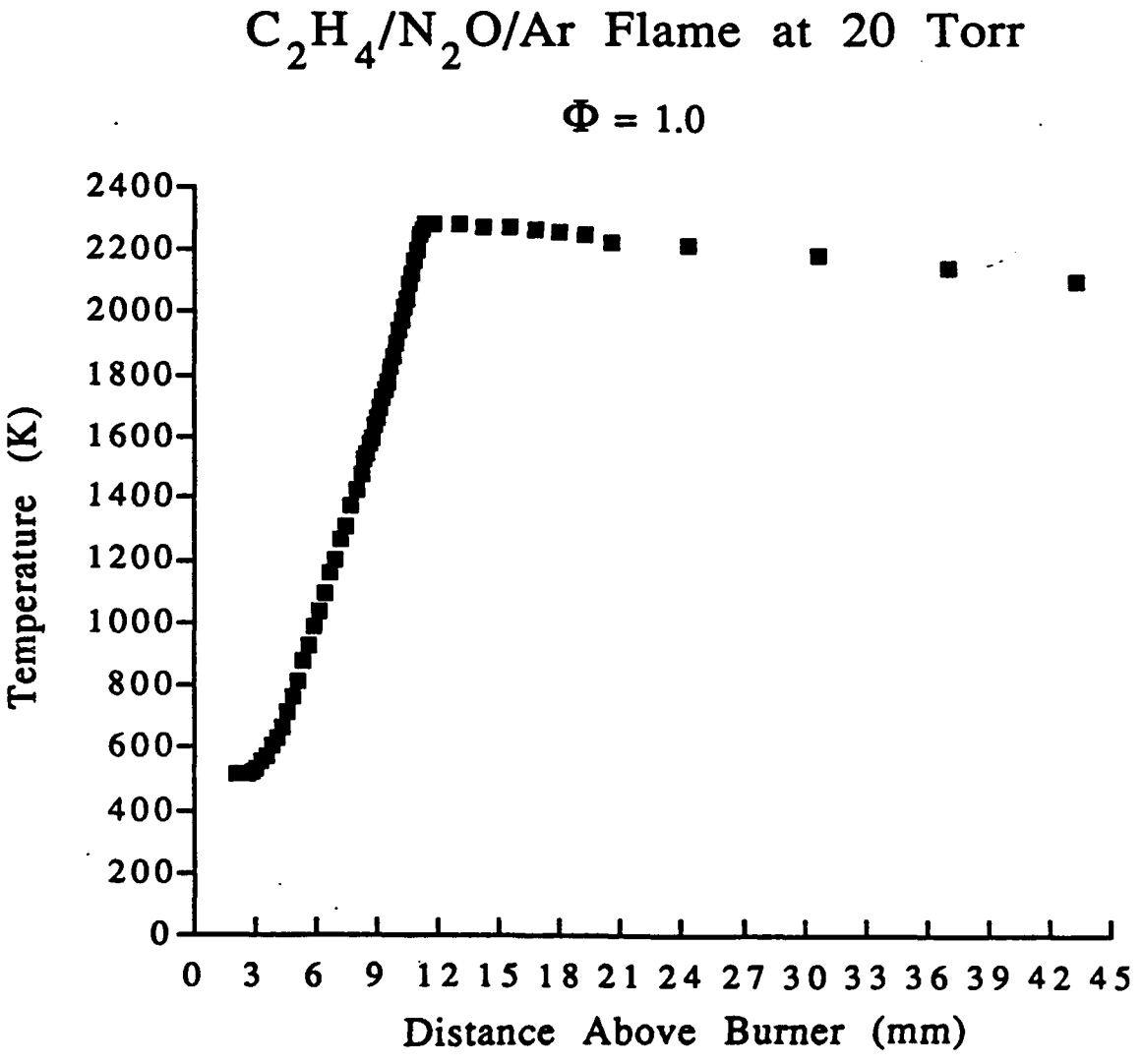

Figure 2. Temperature Profile of $C_2H_4/N_2O/Ar$ Flame, Φ = 1, at 20 Torr.

premixed $C_2H_4/N_2O/Ar$ flame at 20.0 Torr. The temperature profile of the flame in Figure 2 was obtained with a 125-micron diameter Pt/Pt(10%Rh) thermocouple. The thermocouple wire in the flame was coated with a noncatalytic coating as described in the Experimental Section in order to avoid catalytic heating on the thermocouple that would otherwise lead to erronous temperatures and/or break the thermocouple due to localized heating. After coating, the temperatures obtained were corrected for radiative heat losses.

This correction was approximated by equating the heat transferred to the thermocouple from the gases to that lost by radiation. The corrective term is given by (Hayhurst and Kittelson 1977, Peterson 1981)

$$\Delta T = T_{cal} - T_{obs} = \varepsilon\sigma d(T_{obs}^4 - T_o^4)/2k \qquad (4)$$

where ε is the emissivity of the coated thermocouple [taken to be 0.6 (Peterson 1981)], σ is the Stefan-Boltzmann constant, d is the diameter of the junction, k is the thermal conductivity of the gases present at the sampling region (usually approximated with values for air) and T_o is approximately 300 K. The actual thermal conductivity at each point in the flame was obtained as a function of temperature using empirical expressions (Liley and Gambill 1973) and corrected for gas composition as measured in this study. The value of k for the gas mixture varied from 8.41×10^{-5} to 4.09×10^{-4} cal sec^{-1} cm^{-1} K^{-1}. The diameter of the coated thermocouples was measured at 190 microns. The uncertainty in temperature measurements was estimated to be 50 K in the region of peak temperature and 10 K in the preheat region.

The temperature profile in Figure 2 clearly demonstrates flame gas temperatures near the burner surface (about 510 K) that are in excess of that measured by the imbedded thermocouples (about 310 K). Currently, this condition is not included in present theoretical flame models. The region between 0 and approximately 6 mm above the surface is typical of the "dark" or preheat zone of the flame. From 6 to 12 mm the major flame chemistry occurs. This region of steep temperature gradient also contains the visible luminous zone (a light purple or violet color). Above 15 mm is the burnt gas region. This region is on average the hottest region of the flame and is in partial equilibrum with product concentrations near stabilization. Major flame intermediates such as H-atom, O-atom and OH are still in abundance (Howard et al. 1992b). Measurements were not continued until their disappearance since one-dimensionality of the flame at extended distances above the burner surface is not expected.

Further evidence of the major reactivity zone from 6 to 12 mm is the concentration profiles of major radical species. Figures 3 and 4 exhibit several such profiles. Figure 3 shows profiles for H, O and OH. These species form a cadre of important flame radicals that are present in virtually all flames and have been studied in many different flames. They are formed early in the combustion and persist well into the burnt gas region. The peak near 5 mm in the OH profile has been noted for other flames (Howard et al. 1992b) and is found in approximately the lower half of the luminous zone of the flame. This feature may be attributed to competition between the high temperature formation of OH via the following chain-branching reactions,

$$H + O_2 \rightarrow O + OH \qquad (5)$$

and

$$O + H_2 \rightarrow H + OH \qquad (6)$$

with the three body reactions of

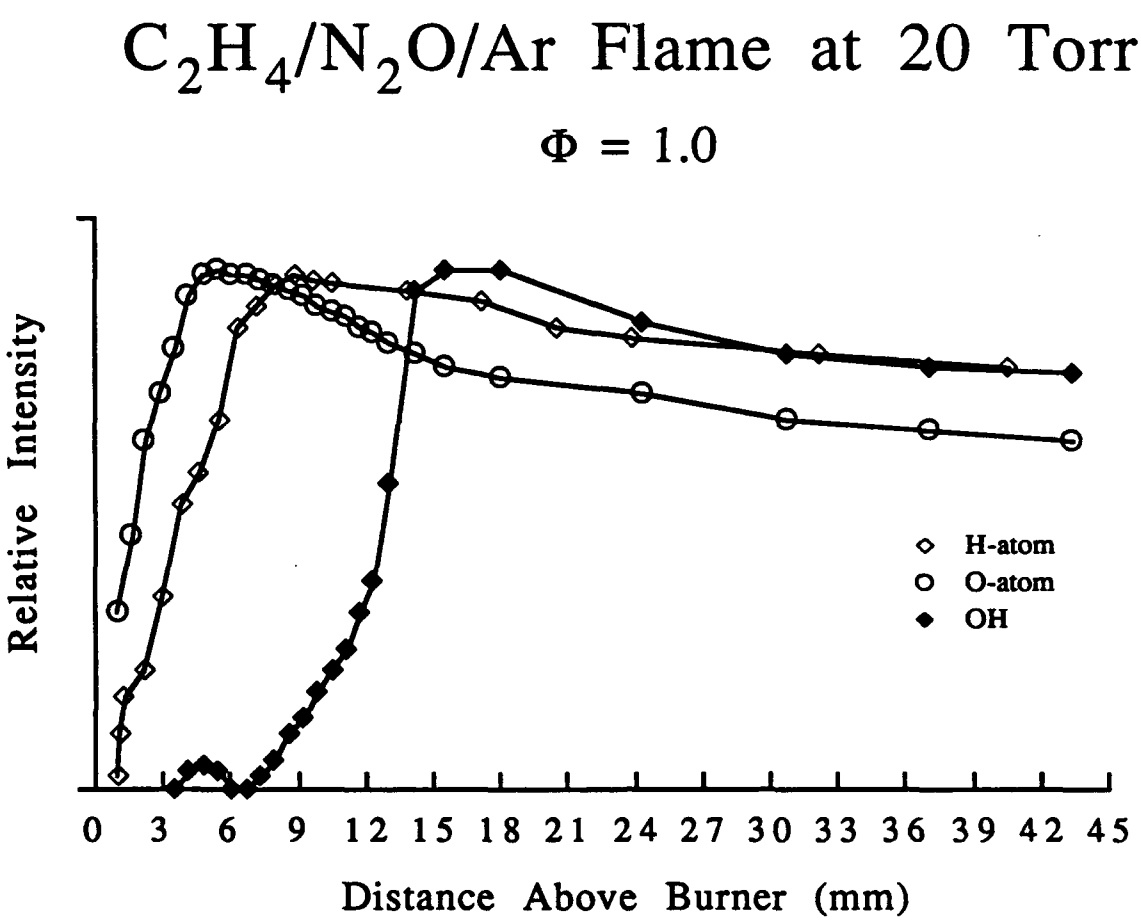

Figure 3. Profiles of H-atom (◇), O-atom (O) and OH (◆) Intermediates of Stoichiometric $C_2H_4/N_2O/Ar$ Flame at 20 Torr. Individual Profiles Normalized to Unity.

$$H + O_2 + M \rightarrow HO_2 + M \qquad (7)$$

and

$$HO_2 + H + M \rightarrow 2OH + M \qquad (8)$$

which are favored at lower temperature (Warnatz 1978). Modelling has yet to be done to confirm the mechanism for this particular flame.

Radicals produced solely by fuel gases appear near the preheat zone, reach their maximum value and disappear within the luminous zone. In Figure 4, the intermediates most closely related to the primary fuel occur first. Their concentrations increase rapidly in the preheat zone,

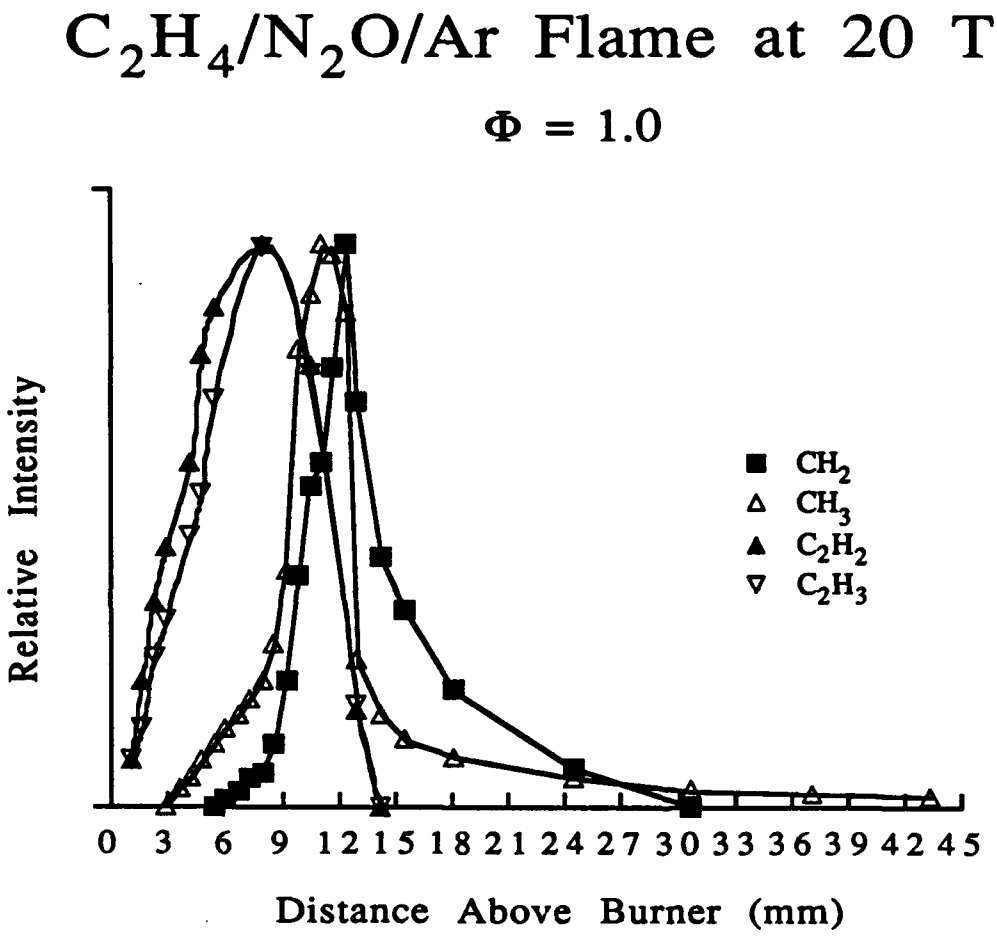

Figure 4. Profiles of Major Hydrocarbon Intermediates of Stoichiometric $C_2H_4/N_2O/Ar$ Flame at 20 Torr. Individual Profiles Normalized to Unity.

begin to diminish as the primary fuel is exhausted and disappear near the top of the luminous zone. As concentrations of C_2H_2 and C_2H_3 increase, one of their fragments, CH_3, is formed. This profile is in turn closely followed by CH_2. These two radicals exist primarily in or just above the luminous zone.

Profiles of stable species where mass assignment is not ambiguous are reported in Figure 5. These species are all flame products. NO and O_2 appear to be produced by predominately high temperature reactions in the upper regions of the luminous zone.

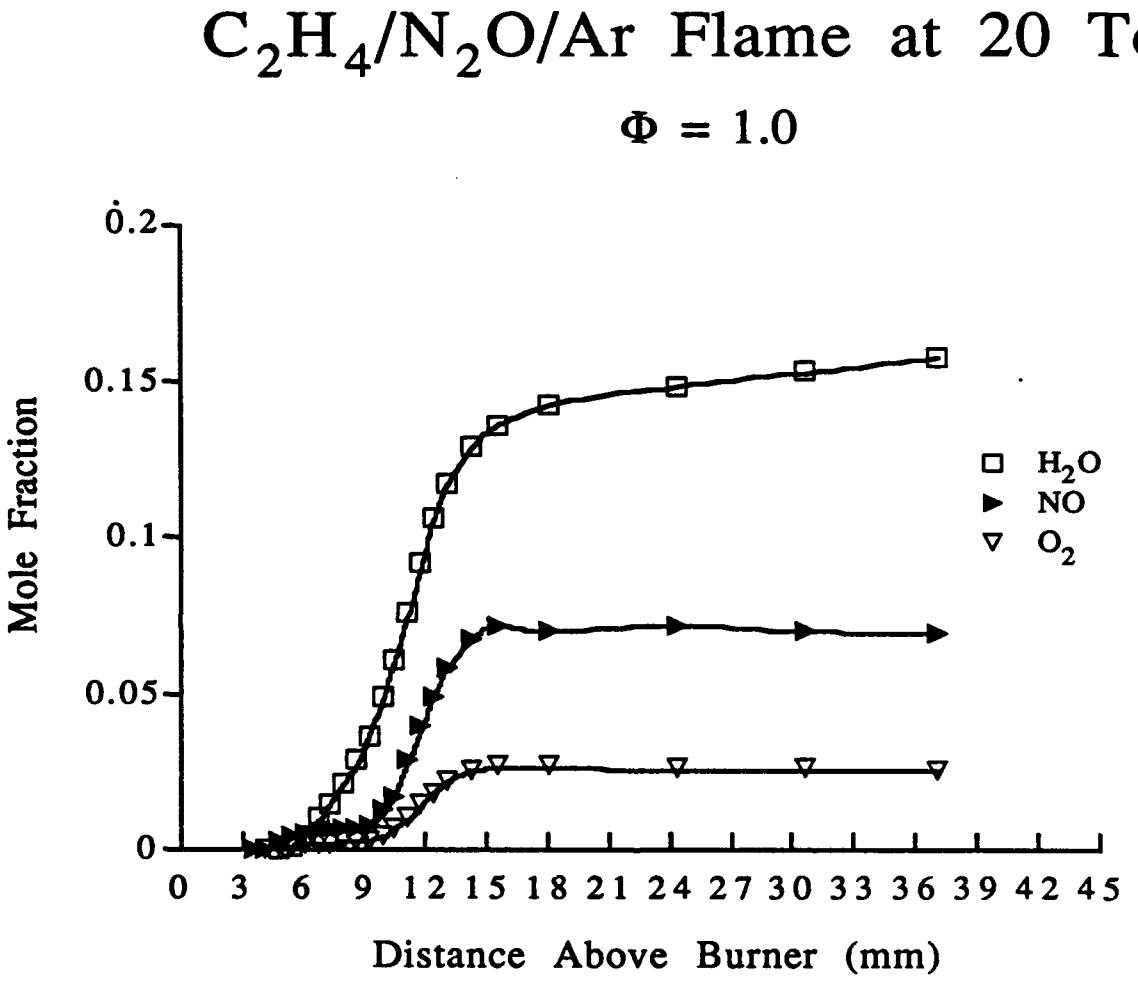

Figure 5. Profiles of H_2O, NO and O_2 in Stoichiometric $C_2H_4/N_2O/Ar$ Flame at 20 Torr. Concentrations Listed in Mole Fraction.

Essentially none of these two products appears below 2000 K, (see Figure 2) and both reach maximum concentration near 2300 K. Since O_2 appears just after NO and has the same profile shape, it is likely that it is produced by the following high-temperature reaction (Coffee 1986):

$$NO + O \rightarrow N + O_2 \quad . \qquad (9)$$

Figure 6 shows total ion currents observed at nominal m/z = 28.0 and 44.0 (each profile normalized to unity). These profiles show the sum of the concentrations of all species at these masses. As shown, little information is available prior to utilizing CID to differentiate between species. However, it is informative to note

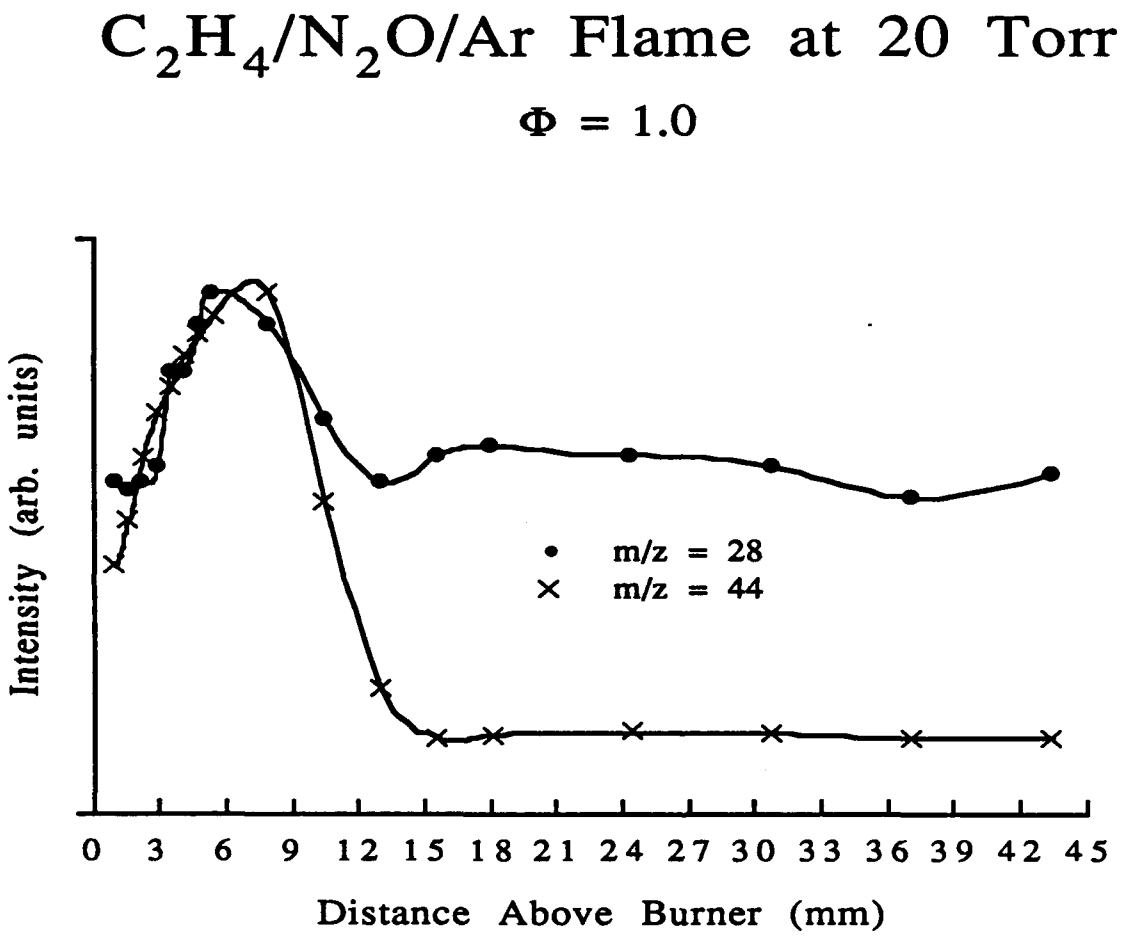

Figure 6. Total Observed Ion Signals at m/z = 28 and 44 for Stoichiometric $C_2H_4/N_2O/Ar$ Flame at 20 Torr.

that both profiles increase during the preheat region (with some initial lag of m/z = 28.0), maximize in the luminous zone, diminish and rapidly achieve a steady state. It should be noted that each profile is the sum of at least two species of differing sensitivity factors (differences of up to a factor of 5 are possible) and corresponding concentrations. The experiment was therefore

repeated at m/z = 28 and 44, this time utilizing the entire triple quadrupole mass filter with collision gas present in the second

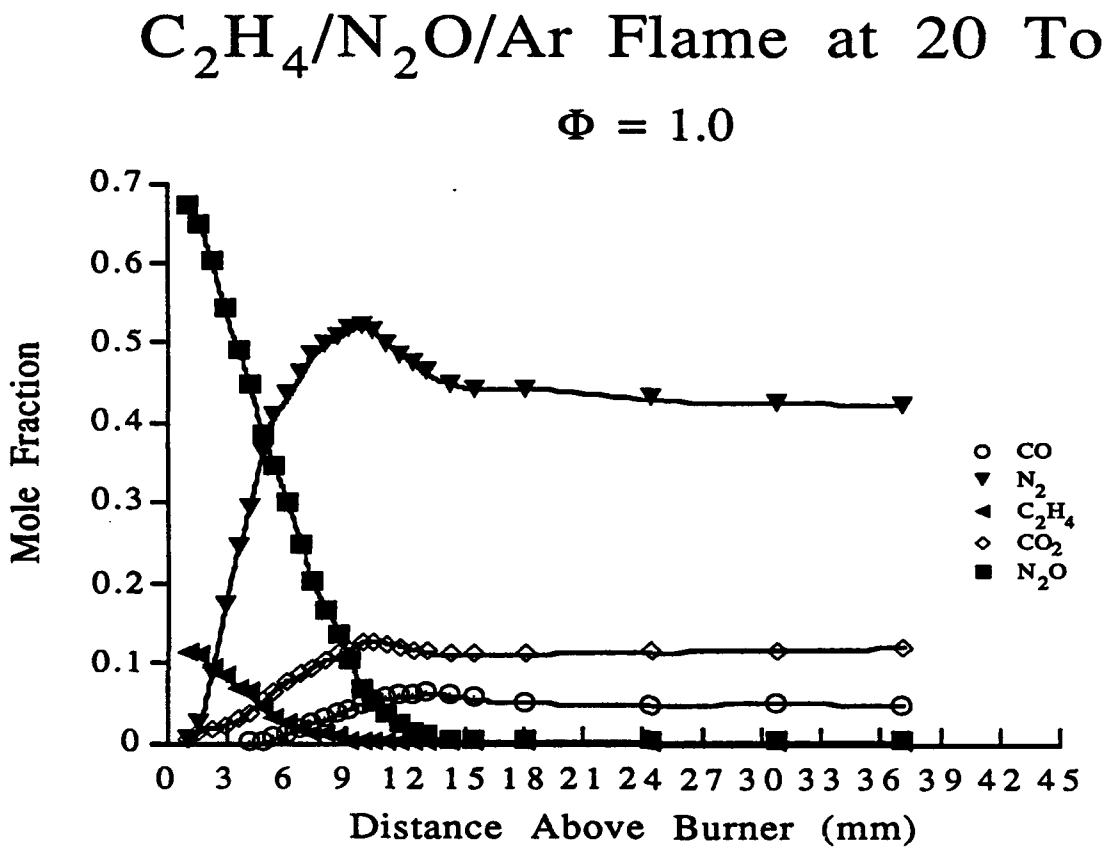

Figure 7. Concentration Profiles (in Mole Fraction) of Species Found by CID at m/z = 28 and 44 in Stoichiometric $C_2H_4/N_2O/Ar$ Flame at 20 Torr. Compare to Total Ion Signals Prior to CID in Figure 6.

quadrupole. The mole fraction of each gas was then obtained from Equation 3 using sensitivity factors obtained during calibration.

Comparison of Figure 6 with Figure 7 demonstrates the utility of using CID to obtain the identity of flame species at the same nominal mass. The progress of the reaction is now easily traced by looking at the consumption of reactants and the evolution of major products (for profile of other products see Figure 4).

3.2 Comparison with the $C_2H_4/O_2/Ar$ Flame. The $C_2H_4/O_2/Ar$ flame has been discussed in another report (Howard et al., 1992b) and only its salient features are discussed here. As a primary comparison of the flames, the temperature profiles are shown in Figure 8. These temperature profiles clearly demonstrates flame gas

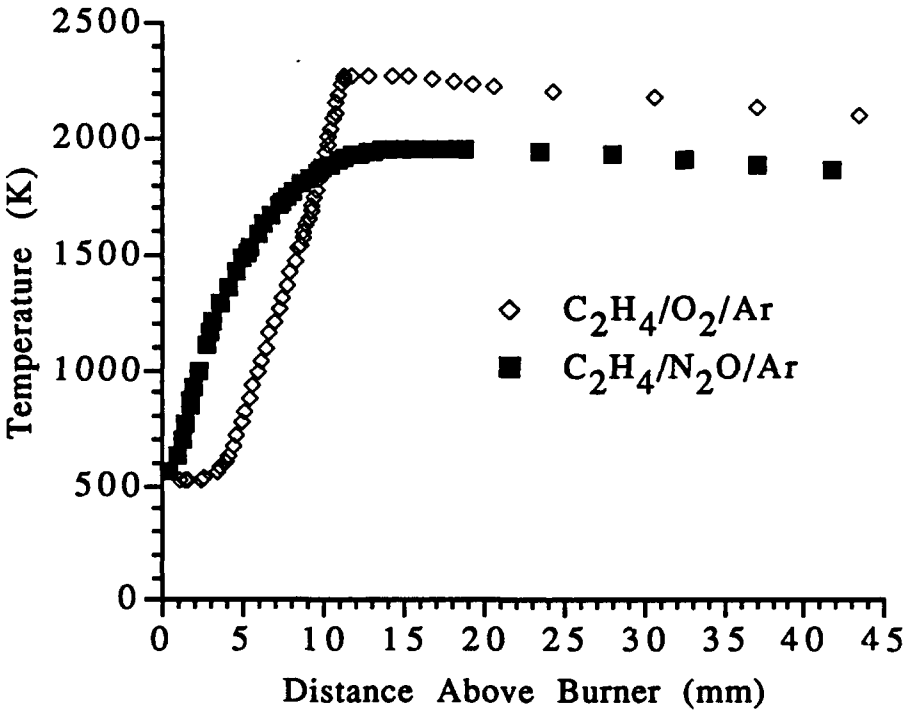

Figure 8. Temperature Profile of $C_2H_4/N_2O/Ar$ and $C_2H_4/O_2/Ar$ Flames, Φ = 1 at 20 Torr.

temperatures near the burner surface (about 500 K) that are in excess of that measured by the imbedded thermocouples (about 310 K) for both flames.

Even though the luminous zones of both flames are comparable, differences are noted in the temperature profiles that indicate dramatically different flame structure. The $C_2H_4/O_2/Ar$ flame has a very short period (less than 2 mm) before the temperature increases rapidly. The comparable period for $C_2H_4/N_2O/Ar$ is more than

double. It was noted in other flames that long induction periods indicate that the flame is near blow-off and the burner does little to stabilize the flame. The fact that the flame does stabilize above the burner and that the luminous zone was flat and comparable in thickness to that of the other flame indicates that the flame speed for $C_2H_4/N_2O/Ar$ is greater than that for $C_2H_4/O_2/Ar$.

Shortly after the induction period, the temperature gradient increases for both flames. $C_2H_4/N_2O/Ar$ increases most dramatically and finally achieves a higher temperature (2300 K versus 1960 K) than the $C_2H_4/O_2/Ar$ flame at approximately the same distance above the burner. After the peak temperature is attained in both flames, the temperature remains essentially constant and then decreases slowly (temperatures typically decrease high in the burnt gas region due to radiative and other heat losses not involving the flame).

Further evidence of the difference in flame structure is found in the concentration profiles of major radical species. Figure 9 exhibits a comparison of profiles for H, O and OH. These species are formed early in both flames and persist well into the burnt gas region for both flames.

The peak near 3 mm (for $C_2H_4/O_2/Ar$) and 5 mm (for $C_2H_4/N_2O/Ar$) in the OH profile is found in approximately the lower half of the luminous zone of the flame. A similar feature is also noted for the O-atom profile for $C_2H_4/O_2/Ar$ at the same distance as the OH profile for the same flame. It is likely that a similar feature for the O-atom profile for $C_2H_4/N_2O/Ar$ is not evident because additional chemistry mechanisms (as explained below) affect production of this radical at low temperatures and outweigh the contribution of Equations 5 and 6. In $C_2H_4/N_2O/Ar$ little O_2 or H_2 is present at the burner surface although concentrations do increase later in the flame (Howard, et al. 1992b). The peaks were also tested

by collision-induced dissociation to determine if they were due to contribution of other species at the same nominal mass as O-atom or OH. These results were negative for other species other than that indicated.

While the H-atom profiles are comparable for both flames, significant differences are noted for both O-atom and OH. For $C_2H_4/O_2/Ar$, the profiles of all three species have the same overall shape and occur at approximately the same distance above the burner. $C_2H_4/N_2O/Ar$, on the other hand, demonstrates profiles that are well-separated in distance. As mentioned earlier, the H-atom profile occurs at essentially the same location as in the sister flame, $C_2H_4/O_2/Ar$. The OH profile, however, is shifted to higher distances above the burner and tracks more closely the temperature profile (as expected). The O-atom profile, on the other hand, is shifted to lower distances above the burner. The early appearance and peaking of the profile can be explained by the presence of N_2O as the primary oxidizer. It has been determined in other N_2O oxidizer flames that the reaction (Anderson 1992)

$$N_2O + M \rightarrow N_2 + M + O \qquad (10)$$

is instrumental in producing O-atom. As the temperature increases, this reaction is accelerated, however, N_2O concentration is being depleted rapidly after 6 mm (Howard et al. 1992c) and other reactions such as Equation 9 that occur to any extent only at high temperatures (i. e., above 2000 K or above 10 mm) also utilize O-atom and diminish the concentration until partial equilibrium is established well into the burnt gas region.

4. SUMMARY

Molecular-beam mass spectrometry with a triple quadrupole mass spectrometer was used to determine concentration profiles

(both relative and absolute, when possible) for all major and most minor flame species (both stable and radical) in the $C_2H_4/N_2O/Ar$ flame at 20 Torr. Collision-induced dissociation of initial ions at m/z = 28 and 44 enabled resolution of the primary ion signal into the contributions of the various species present at these nominal masses. The combustion history of the flame was then clearly evident in the consumption of reactants and appearance of products. Minor flame products CO, NO and O_2 were also noted. Appearance of products was also correlated with temperature profile obtained by thermocouple.

This flame was compared to the $C_2H_4/O_2/Ar$ flame. Temperature and species concentration profiles for H-atom, O-atom and OH were compared. Collision-induced dissociation of initial ions at m/z = 16 and 17 verified the identity of O-atom and OH, respectively. H-atom profiles were essentially the same in both flames, with O-atom and OH profiles for $C_2H_4/O_2/Ar$ nearly coincident with H-atom. For $C_2H_4/N_2O/Ar$, O-atom production was accelerated early in the flame and diminished until a nearly constant level was established. In the same flame, OH appeared much later than H-atom and more nearly coincided with the temperature profile as obtained by thermocouple measurements.

5. REFERENCES

Alden, M., Edner, H., Grafstrom, P., and Svanberg, S., Optics Commun. Vol. 42, p. 244, 1982.

Anderson, W. R., US Army Ballistic Research Laboratory, private communication, 1992.

Banna, S. M., PhD Thesis, University of California, Berkeley, 1979.

Biordi, J. C., Lazzara, C. P. and Papp, J. F., Combust. Flame, Vol. 23, p. 73, 1974.

Coffee, T. P., Combust. Flame, Vol 65, p. 53, 1986.

Colket, III, M. B., Chiappetta, L., Guile, R. N., Zabielski, M. F., Seery, D. J., Combust. Flame, Vol. 44, p. 3, 1982.

Eltenton, G. C., J. Chem. Phys., Vol. 15, p. 455, 1947.

Fristrom, R. M.; Westenberg, A. A., Flame Structure, McGraw-Hill, New York 1965.

Gaydon, A. G. and Wolfhard, H. G., Third Symposium (Int.) Combustion and Explosion Phenomena, Williams & Wilkins, Baltimore 1949; p. 504.

Goldsmith, J. E. M., J. Chem. Phys., Vol 78, p. 1610, 1983.

Greene, H. A. and Pust, H., Anal. Chem., Vol. 30, p. 1039, 1958.

Hayhurst, A. N. and Kittelson, D. B., Combust. Flame, Vol. 28, p. 301, 1977.

Howard, S. L., Locke, R. J., Sausa, R. C. and Miziolek, A. W., Rapid Commun. Mass Spectrum., accepted for publication, Feb. 1992.

Howard, S. L., Locke, R. J., Sausa, R. C. and Miziolek, A. W., U. S. Army Ballistic Research Laboratory Technical Report, BRL-TR-3328, April 1992.

Howard, S. L., Newberry, J., Sausa, R. C. and Miziolek, A. W., J. Amer. Soc. Mass Spectrum., submitted, Jan 1992.

Kent, J. H., Combust. Flame, Vol. 14, p. 279, 1970.

Knewstubb, P. F. and Sugden, T. M., Nature, Vol. 181, p. 1261, 1958.

Liley, P. E., Gambill, W. R., In Chemical Engineer's Handbook, 5th ed.; Perry, R. H. and Chilton, C. H., Eds.; McGraw-Hill, New York 1973, Section 3.

Lucht, R. P., Salmon, J. T., King, G. B., Sweeney, D. W., and Laurendeau, N. M., Optics Lett., Vol. 8, p. 365, 1983.

Peterson, R. C., PhD Thesis, Purdue University, 1981.

Revet, J. M., Puechberty, D. and Cottereau, M. J., Combust. Flame, Vol. 33, p. 5, 1978.

Salmon, J. T. and Laurendeau, N. M., Applied Optics, Vol. 26, p. 2881, 1987.

Seery, D. J. and Zabielski, M. F., Combust. Flame, Vol. 78, p. 169, 1989.

Smith, O. I. and Chandler, D. W., Combust. Flame, Vol. 63, p. 19, 1986.

Smith, O. I., Combust. Flame, Vol. 40, p. 187, 1981.

Warnatz, J., Ber. Bunsenges. Phys. Chem., Vol. 82, p. 834, 1978.

INTENTIONALLY LEFT BLANK.

No. of Copies	Organization
2	Administrator Defense Technical Info Center ATTN: DTIC-DDA Cameron Station Alexandria, VA 22304-6145
1	Commander U.S. Army Materiel Command ATTN: AMCAM 5001 Eisenhower Ave. Alexandria, VA 22333-0001
1	Commander U.S. Army Laboratory Command ATTN: AMSLC-DL 2800 Powder Mill Rd. Adelphi, MD 20783-1145
2	Commander U.S. Army Armament Research, Development, and Engineering Center ATTN: SMCAR-IMI-I Picatinny Arsenal, NJ 07806-5000
2	Commander U.S. Army Armament Research, Development, and Engineering Center ATTN: SMCAR-TDC Picatinny Arsenal, NJ 07806-5000
1	Director Benet Weapons Laboratory U.S. Army Armament Research, Development, and Engineering Center ATTN: SMCAR-CCB-TL Watervliet, NY 12189-4050
(Unclass. only) 1	Commander U.S. Army Rock Island Arsenal ATTN: SMCRI-TL/Technical Library Rock Island, IL 61299-5000
1	Director U.S. Army Aviation Research and Technology Activity ATTN: SAVRT-R (Library) M/S 219-3 Ames Research Center Moffett Field, CA 94035-1000
1	Commander U.S. Army Missile Command ATTN: AMSMI-RD-CS-R (DOC) Redstone Arsenal, AL 35898-5010

No. of Copies	Organization
1	Commander U.S. Army Tank-Automotive Command ATTN: ASQNC-TAC-DIT (Technical Information Center) Warren, MI 48397-5000
1	Director U.S. Army TRADOC Analysis Command ATTN: ATRC-WSR White Sands Missile Range, NM 88002-5502
1	Commandant U.S. Army Field Artillery School ATTN: ATSF-CSI Ft. Sill, OK 73503-5000
2	Commandant U.S. Army Infantry School ATTN: ATZB-SC, System Safety Fort Benning, GA 31903-5000
(Class. only) 1	Commandant U.S. Army Infantry School ATTN: ATSH-CD (Security Mgr.) Fort Benning, GA 31905-5660
(Unclass. only) 1	Commandant U.S. Army Infantry School ATTN: ATSH-CD-CSO-OR Fort Benning, GA 31905-5660
1	WL/MNOI Eglin AFB, FL 32542-5000
	Aberdeen Proving Ground
2	Dir, USAMSAA ATTN: AMXSY-D AMXSY-MP, H. Cohen
1	Cdr, USATECOM ATTN: AMSTE-TC
3	Cdr, CRDEC, AMCCOM ATTN: SMCCR-RSP-A SMCCR-MU SMCCR-MSI
1	Dir, VLAMO ATTN: AMSLC-VL-D
10	Dir, USABRL ATTN: SLCBR-DD-T

No. of Copies	Organization
4	Commander U.S. Army Research Office ATTN: R. Ghirardelli D. Mann R. Singleton R. Shaw P.O. Box 12211 Research Triangle Park, NC 27709-2211
2	Commander U.S. Army Armament Research, Development, and Engineering Center ATTN: SMCAR-AEE-B, D. S. Downs SMCAR-AEE, J. A. Lannon Picatinny Arsenal, NJ 07806-5000
1	Commander U.S. Army Armament Research, Development, and Engineering Center ATTN: SMCAR-AEE-BR, L. Harris Picatinny Arsenal, NJ 07806-5000
1	Office of Naval Research Department of the Navy ATTN: R. S. Miller, Code 432 800 N. Quincy Street Arlington, VA 22217
5	Commander Naval Research Laboratory ATTN: M. C. Lin J. McDonald E. Oran J. Shnur R. J. Doyle, Code 6110 Washington, DC 20375
1	Superintendent Naval Postgraduate School Dept. of Aeronautics ATTN: D. W. Netzer Monterey, CA 93940
1	AFOSR ATTN: J. M. Tishkoff Bolling Air Force Base Washington, DC 20332

No. of Copies	Organization
1	NASA Langley Research Center Langley Station ATTN: G. B. Northam/MS 168 Hampton, VA 23365
1	Aerojet Solid Propulsion Co. ATTN: P. Micheli Sacramento, GA 95813
1	Applied Combustion Technology, Inc. ATTN: A. M. Varney P.O. Box 607885 Orlando, FL 32860
1	AVCO Everett Research Laboratory Division ATTN: D. Stickler 2385 Revere Beach Parkway Everett, MA 02149
1	Battelle ATTN: TACTEC Library, J. N. Huggins 505 King Ave. Columbus, OH 43201-2693
1	Battelle Northwest Laboratories ATTN: A. L. Rockwood, MS P-8-19 P.O. Box 999 Richland, WA 99352
1	Dow Chemical U.S.A. Analytical Sciencies, Thermal Group ATTN: S. W. Froelicher 1897 Building Midland, MI 48667
1	Exxon Research & Eng. Co. ATTN: A. Dean Route 22E Annandale, NJ 08801
1	General Applied Science Laboratories, Inc. 77 Raynor Avenue Ronkonkama, NY 11779-6649

No. of Copies	Organization
1	General Electric Ordnance Systems ATTN: J. Mandzy 100 Plastics Avenue Pittsfield, MA 01203
1	General Motors Rsch Labs Physical Chemistry Department ATTN: Tom Sloane Warren, MI 48090-9055
2	Hercules, Inc. Allegheny Ballistics Lab. ATTN: W. B. Walkup E. A. Yount P.O. Box 210 Rocket Center, WV 26726
1	Alliant Techsystems, Inc. ATTN: R. E. Tompkins MS MN38-33300 5700 Smetana Drive Hopkins, MN 55343
1	IIT Research Institute ATTN: R. F. Remaly 10 West 35th Street Chicago, IL 60616
2	Director Lawrence Livermore National Laboratory ATTN: C. Westbrook M. Costantino P.O. Box 808 Livermore, CA 94550
1	Lockheed Missiles & Space Co. ATTN: George Lo 3251 Hanover Street Dept. 52-35/B204/2 Palo Alto, CA 94304
1	Los Alamos National Laboratory ATTN: B. Nichols, T7, MS-B284 P.O. Box 1663 Los Alamos, NM 87545

No. of Copies	Organization
1	Olin Ordnance ATTN: V. McDonald, Library P.O. Box 222 St. Marks, FL 32355-0222
1	Paul Gough Associates, Inc. ATTN: P. S. Gough 1048 South Street Portsmouth, NH 03801-5423
2	Princeton Combustion Research Laboratories, Inc. ATTN: M. Summerfield N. A. Messina 475 U.S. Highway One Monmouth Junction, NJ 08852
1	Hughes Aircraft Company ATTN: T. E. Ward 8433 Fallbrook Ward Canoga Park, CA 91303
2	Rockwell International Corp. Rocketdyne Division ATTN: J. E. Flanagan/HB02 T. L. Bunn 6633 Canoga Avenue Canoga Park, CA 91304
4	Director Sandia National Laboratories Division 8354 ATTN: R. Cattolica S. Johnston P. Mattern D. Stephenson Livermore, CA 94550
1	Science Applications, Inc. ATTN: R. B. Edelman 23146 Cumorah Crest Woodland Hills, CA 91364
3	SRI International ATTN: G. Smith D. Crosley D. Golden 333 Ravenswood Avenue Menlo Park, CA 94025

No. of Copies	Organization
1	Stevens Institute of Tech. Davidson Laboratory ATTN: R. McAlevy III Hoboken, NJ 07030
1	Sverdrup Technology, Inc. LERC Group ATTN: R. J. Locke, MS SVR-2 2001 Aerospace Parkway Brook Park, OH 44142
1	Thiokol Corporation Elkton Division ATTN: S. F. Palopoli P.O. Box 241 Elkton, MD 21921
3	Thiokol Corporation Wasatch Division ATTN: S. J. Bennett P.O. Box 524 Brigham City, UT 84302
1	United Technologies Research Center ATTN: A. C. Eckbreth East Hartford, CT 06108
3	United Technologies Corp. Chemical Systems Division ATTN: R. S. Brown T. D. Myers (2 copies) P.O. Box 49028 San Jose, CA 95161-9028
1	Universal Propulsion Company ATTN: H. J. McSpadden 25401 North Central Ave. Phoenix, AZ 85027-7837
1	Veritay Technology, Inc. ATTN: E. B. Fisher 4845 Millersport Highway P.O. Box 305 East Amherst, NY 14051-0305
1	Brigham Young University Dept. of Chemical Engineering ATTN: M. W. Beckstead Provo, UT 84058

No. of Copies	Organization
1	California Institute of Tech. Jet Propulsion Laboratory ATTN: L. Strand, MS 512/102 4800 Oak Grove Drive Pasadena, CA 91109
1	California Institute of Technology ATTN: F. E. C. Culick/MC 301-46 204 Karman Lab. Pasadena, CA 91125
1	University of California Los Alamos Scientific Laboratory P.O. Box 1663, Mail Stop B216 Los Alamos, NM 87545
2	University of California, Santa Barbara Quantum Institute ATTN: K. Schofield M. Steinberg Santa Barbara, CA 93106
1	University of Colorado at Boulder Engineering Center ATTN: J. Daily Campus Box 427 Boulder, CO 80309-0427
2	University of Southern California Dept. of Chemistry ATTN: S. Benson C. Wittig Los Angeles, CA 90007
1	Cornell University Department of Chemistry ATTN: T. A. Cool Baker Laboratory Ithaca, NY 14853
1	University of Delaware ATTN: A. K. Shukla Department of Chemistry Newark, DE 19716
1	University of Delaware ATTN: T. Brill Chemistry Department Newark, DE 19711

No. of Copies	Organization
1	University of Florida Dept. of Chemistry ATTN: J. Winefordner Gainesville, FL 32611
3	Georgia Institute of Technology School of Aerospace Engineering ATTN: E. Price W. C. Strahle B. T. Zinn Atlanta, GA 30332
1	Johns Hopkins University/APL Chemical Propulsion Information Agency ATTN: T. W. Christian Johns Hopkins Road Laurel, MD 20707
1	University of Michigan Gas Dynamics Lab Aerospace Engineering Lab ATTN: G. M. Faeth Ann Arbor, MI 48109-2140
3	Pennsylvania State University Applied Research Laboratory ATTN: K. K. Kuo H. Palmer M. Micci University Park, PA 16802
2	Purdue University School of Mechanical Engineering ATTN: N. M. Laurendeau S. N. B. Murthy TSPC Chaffee Hall West Lafayette, IN 47906
1	Rensselaer Polytechnic Inst. Dept. of Chemical Engineering ATTN: A. Fontijn Troy, NY 12181
1	University of Texas Dept. of Chemistry ATTN: W. Gardiner Austin, TX 78712

INTENTIONALLY LEFT BLANK.

USER EVALUATION SHEET/CHANGE OF ADDRESS

This laboratory undertakes a continuing effort to improve the quality of the reports it publishes. Your comments/answers below will aid us in our efforts.

1. Does this report satisfy a need? (Comment on purpose, related project, or other area of interest for which the report will be used.) _____

2. How, specifically, is the report being used? (Information source, design data, procedure, source of ideas, etc.) _____

3. Has the information in this report led to any quantitative savings as far as man-hours or dollars saved, operating costs avoided, or efficiencies achieved, etc? If so, piease elaborate. _____

4. General Comments. What do you think should be changed to improve future reports? (Indicate changes to organization, technical content, format, etc.) _____

BRL Report Number BRL-TR-3352 Division Symbol _____

Check here if desire to be removed from distribution list. ____

Check here for address change. ____

Current address: Organization _____
Address _____

DEPARTMENT OF THE ARMY
Director
U.S. Army Ballistic Research Laboratory
ATTN: SLCBR-DD-T
Aberdeen Proving Ground, MD 21005-5066

OFFICIAL BUSINESS

BUSINESS REPLY MAIL
FIRST CLASS PERMIT No 0001, APG, MD

Postage will be paid by addressee.

Director
U.S. Army Ballistic Research Laboratory
ATTN: SLCBR-DD-T
Aberdeen Proving Ground, MD 21005-5066

NO POSTAGE
NECESSARY
IF MAILED
IN THE
UNITED STATES